Palaeogeography, Palaeoclimatology, Palaeoecology 281 (2009) 334–344

Contents lists available at ScienceDirect

Palaeogeography, Palaeoclimatology, Palaeoecology

journal homepage: www.elsevier.com/locate/palaeo

Long-term glacier variations in the Central Andes of Argentina and Chile, inferred from historical records and tree-ring reconstructed precipitation

Carlos Le Quesne [a,*], Cesar Acuña [b], José A. Boninsegna [c], Andrés Rivera [b,d], Jonathan Barichivich [a]

[a] Laboratorio de Dendrocronología, Facultad de Ciencias Forestales, Universidad Austral de Chile, casilla 567 Valdivia, Chile
[b] Glaciología y Cambio Climático, Centro de Estudios Científicos, Arturo Prat 514, Valdivia, Chile
[c] Instituto Argentino de Nivología, Glaciología y Ciencias Ambientales, Ruiz Leal s/n Parque San Martín (5500), Mendoza, Argentina
[d] Departamento de Geografía, Universidad de Chile, Marcoleta 250, Santiago, Chile

ARTICLE INFO

Article history:
Received 11 July 2007
Accepted 18 January 2008
Available online 7 September 2008

Keywords:
Austrocedrus chilensis
Tree-rings
Historical documents
Glacier retreat
Dendroclimatology

ABSTRACT

Snow and ice in the Central Andes of Chile and Argentina (33–36 °S) are the major source of water for the highly populated regions near the cities of Santiago and Mendoza. However, our knowledge of the forces driving the general glacier retreat in the region is limited. In order to obtain a long-term perspective of glacier fluctuations and their relationships with climate in the Central Andes, historical glacier variations were documented and compared with a tree-ring precipitation reconstruction based upon *Austrocedrus chilensis* trees. A multi-proxy approach (historical documents, old aerial photographs and satellite imagery) was used to map the fluctuations of eight glaciers, including the Cipreses Glacier, which provides the oldest record of glacier variations in the region starting in AD 1842. All the studied glaciers exhibited a negative trend during the 20th century with mean frontal retreats between −50 and −9 m y^{-1}, thinning rates between 0.76 and 0.56 m y^{-1} and a mean ice area reduction of 3% since 1955. More than 350 tree-ring cores were combined into three tree-ring chronologies, which strongly correlate with the instrumental precipitation in Santiago de Chile (33°26′ S; 70°41′ W, 520 m asl). Based on these records, a 712-year precipitation reconstruction was developed. This reconstruction is characterised by a centennial oscillation indicating marked dry conditions around the years 1440 and 1600 AD. Wet conditions were prevalent in the years 1500, 1650 and particularly around 1850 AD. Since this precipitation maximum, the reconstruction shows a clear, secular, decreasing trend. The reduction in precipitation indicated by this reconstruction for the last 150 yr, in combination with a significant warming recorded in Central Chile, are the main causes of the observed current glacier retreats.

1. Introduction

Due to its transitional location between subtropical and temperate latitudes, the climate in Central Chile is characterised by a high inter-annual variability in precipitation (Aceituno et al., 1993; Montecinos and Aceituno, 2003; Quintana, 2004). At the end of 1960s and during the 1990s, this region experienced extreme drought events (Quintana, 2000), which seriously affected water consumption, irrigation, and generation of hydroelectric power (Norero and Bonilla, 1999). These natural restrictions in water supply occurred concurrently with higher human pressure on water resources, generating strong competition for water allocation as a result of the regional economic growth (Rosegrant et al., 2000). The drought events in this region are partially correlated to cold phases of ENSO, the so-called La Niña events (Masiokas et al., 2006), which are typically associated with negative glacier mass balances, as opposed to positive glacier mass balances during El Niño events (Escobar and Aceituno, 1998).

Water consumption in this region of Argentina and Chile is highly dependent on snow accumulation and glacial melt, particularly during summers preceded by episodic winter droughts when up to 67% of the water flow of Río Maipo (Peña and Nazarala, 1987) and 70% of the discharge of Río San Juan (Leiva, 1999) has been generated by glacial meltwater. In this regard, and additionally due to recent glacier retreat and wasting ice, runoff from some glaciated Chilean basins has increased (Carrasco et al., 2005). In the long-term, runoff is expected to drop significantly during the dry seasons due to the disappearance of glaciers, in similar fashion to what is currently occurring in the Tropical Andes (Juen et al., 2007).

In spite of the general trend of glacial retreat on both sides of the Andes during the 20th century (Llorens and Leiva, 1995; Leiva, 1999; Rivera et al., 2002), some glaciers experienced sudden advances. This occurred both in Chile during the 1950s (Lliboutry, 1956) and in Argentina during the 1930s, and 1980s, when Glaciar Grande del Nevado del Plomo advanced rapidly, damming a valley and generating two floods (Bruce et al., 1987). Similarly, Glaciar de la Laguna in Río Atuel advanced 1400 m between 1970 and 1982 (Cobos and Boninsegna, 1983). Some of these advances have been related to

* Corresponding author. Fax: +56 63 293418.
E-mail address: clequesn@uach.cl (C. Le Quesne).
URL: http://www.dendrocronologia.cl.

0031-0182/$ – see front matter © 2008 Elsevier B.V. All rights reserved.
doi:10.1016/j.palaeo.2008.01.039

Table 1
Geographical description of studied glaciers.

	Chile				Argentina			
River basin	Cachapoal			Tinguiririca		Atuel		
Glacier name	Cipreses	Cortaderal	Palomo	Universidad	De la Laguna	Humo	Corto	Fiero
Latitude S	34°33'21"	34°38'32"	34°33'12"	34°42'51"	34°31'21"	34°33'59"	34°35'00"	34°36'32"
Longitude W	70°22'10"	70°15'35"	70°16'05"	70°20'53"	70°06'24"	70°07'56"	70°08'20"	70°09'19"
Length (km)*	10.6	9	7.3	10.6	5.2	3.5	3.2	5.4
Total area (km^2)*	35.7	15	14.5	29.2	8.2	10.7	2.2	7.8
General aspect	W	SE	NE	S	S	SE	E	SE
Min. elevation (m)**	2616	2738	2629	2463	3250	3060	3136	2903
Max. elevation (m)**	4365	4845	4478	4543	4338	4089	3945	4014

*Area and length based upon a Landsat ETM+ acquired on January 20, 2000.
** Altitude extracted from SRTM data.

surge events (Leiva, 1999), which are not necessarily responses to climatic changes. In this situation they may be generated by changes in the normal subglacial drainage system, particularly when temperate glaciers are involved, such as in Central Chile and Argentina (Paterson, 1994; Harrison and Post, 2003).

Recent glacial responses in this part of the Andes have previously been related (Rivera et al., 2002) to both atmospheric warming (Rosenblüth et al., 1997) and decreases in precipitation (Quintana, 2004). As yet, little research has been done regarding Holocene glacial responses (e.g., Espizúa, 1993). These long-term variations are useful for understanding how water resources may change in the future as a consequence of predicted temperature and precipitation changes (e. g., IPCC, 2001).

In order to obtain a better insight into the long-term climate variability of this part of the Andes, two independent proxies were used: historical documents on glacier variations and precipitation variability reconstructed by moisture-sensitive tree-ring chronologies. These two proxies allow extension of analysis into the past, for periods where instrumental records are limited or non existent (Bradley et al., 2004).

For this purpose, eight glaciers located in the Cachapoal and Tinguiririca basins in Chile, and the Atuel basin in Argentina were selected (Table 1, Figs. 1 and 2). Most of these glaciers have previously been analysed (e.g., Caviedes, 1979; Cobos and Boninsegna, 1983; Rivera et al., 2006), allowing the reconstruction of long-term variations of frontal glacier tongues. One of the glaciers with the longest historical record of frontal variations is Glaciar Cipreses (34°33′ S; 70°22′ W), whose frontal position was first noted by Domeyko in 1842 (Domeyko, 1978). More recent aerial photographs and satellite images (Table 2) have enabled updating of glacier positions to the year 2007.

Glaciar Cipreses was also chosen for more detailed analysis, due to disjunctive stands of *Austrocedrus chilensis* at lower altitudes in its valley (Ciprés de la Cordillera, Fig. 2). This species has previously been used to provide a proxy record for precipitation in central Chile (Boninsegna, 1988, 1992; Luckman and Villalba, 2001). A robust moisture-sensitive tree-ring network was developed to analyse the long-term precipitation variability during the last seven centuries. This annually-resolved proxy allowed the determination of the leading modes of precipitation variability at different time scales

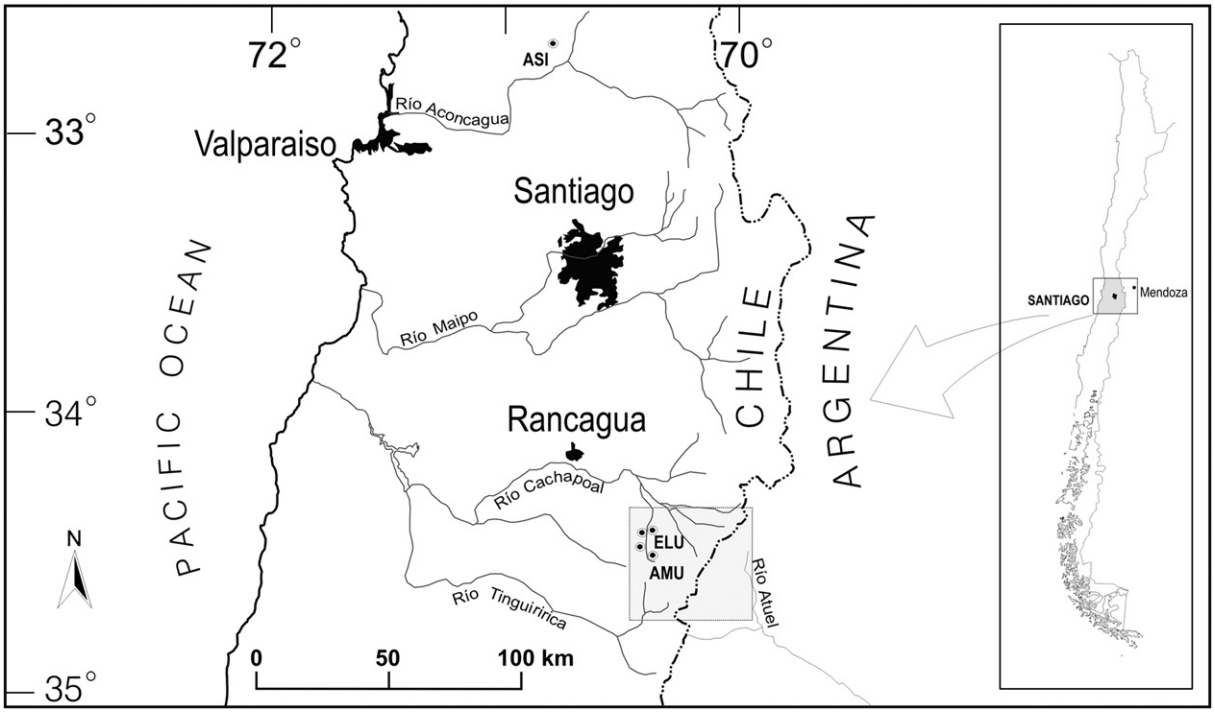

Fig. 1. Map of Central Chile and Argentina showing the study area, main rivers, cities and the *Austrocedrus chilensis* tree-ring sites. Locations of tree-ring chronologies are indicated by black points: ASI, El Asiento in the Río Aconcagua area, and ELU and AMU along the Río Cipreses. The box corresponds to the area covered by the Landsat ETM+ image shown in Fig. 4.

Fig. 2. Moisture-sensitive *Austrocedrus chilensis* (Ciprés de la Cordillera) trees located on steep rocky slopes. These long-lived trees can reach up to 900 yr old. In the background, Glaciar Palomo at the head of Río Cortaderal.

(e.g., inter-annual, decadal/inter-decadal and secular oscillation modes) and enabled inferences on the effect of possible climatic forcing on glacial behaviour (e.g., ENSO).

2. Data and methods

2.1. Glacier variations

Variations in glacial fronts and area were obtained through comparison of geo-located and ortho-rectified satellite images, acquired from 1976 to present (Table 2), where glacier boundaries were digitised on screen based upon colour composite images produced from Landsat MultiSpectral Scanner MSS, Thematic Mapper TM and Enhanced Thematic Mapper Plus ETM+ bands with histogram-equalised stretches. The horizontal errors of these satellite images, after geo-location and ortho-rectification, are within one pixel size (Table 2).

Several aerial photographs (Table 2) were manually analysed with mirror stereoscopes to map the approximate position of the glaciers. The resulting interpretation was then transferred to a 1:50,000 scale regular cartography of the area using a Zoom Transfer Scope analogue instrument, yielding horizontal errors of a couple of tens of metres. The final interpretations were then digitised and incorporated into a Geographical Information System (GIS), where all available data sets were compared, taking into account any temporal changes in glacial characteristics.

The positioning of glacial fronts from historical accounts (prior to 1955) is typically less accurate than using remotely sensed imagery, however, the reports available in the literature provide precious information from a time where very little is known about glacier behaviour. Thus, all historical records were carefully interpreted and compared between available sources, in order to estimate the position of the glacial fronts at specific times. Some of these reports provided a photograph or a sketch map of the glacier; others describe retreats or changes with respect to previous positions. In some accounts the glaciers were only described in terms of minimum altitude or relative position in comparison to a geographically prominent feature (e.g., river confluence), making interpretation more difficult. The positions of the glacier for these historical accounts are considered a first order approximation, within several tens or even a couple of hundred of meters.

The Equilibrium Line Altitudes (ELAs) of the glaciers were determined by the analyses of Landsat ETM+ images acquired in the summer. At the end of the dry season in the Central Andes of Argentina and Chile, the transient snow line is coincident with the ELA due to the temperate condition of the glaciers (Rivera et al., 2000).

Table 2
Remote sensing information used in this study.

	Aerial photographs			
Flight name	Scale	Date	Focal length (mm)	Type
Hykon	1:70,000	Feb 21, 1955	153.62	Vertical
Geotec	1:50,000	Feb 25, 1997	153.17	Vertical
Satellite images				
Sensor	Spatial resolution (m)		Date	Source
Landsat MSS	57×79		Mar 15, 1976	GLCF
Landsat TM	28.5		Feb 9, 1987	GLCF
Landsat ETM+	28.5		Jan 20, 2000	GLCF
Terra ASTER	15		Apr 9, 2003	USGS

2.2. Ice elevation changes

A Digital Elevation Model (DEM) was generated by interpolation of photogrammetrically-derived contour lines (published by Instituto Geográfico Militar (IGM)) of Chile, based upon 1955 Hykon aerial photographs (Table 2). No error estimations for the regular cartography of the IGM are available, however, the regular cartography at 1:50,000 scale is considered to be of class 1 accuracy in terms of the American Society for Photogrammetry and Remote Sensing classification (Falkner, 1995). This cartography is therefore, most precise, with vertical inaccuracies related to the contour interval (25 m) possessing a vertical error of 17 m. After applying several interpolation methods, a jack-knifing procedure (Lythe et al., 2001) allowed determination of the DEM of best fit, yielding 9 m of vertical random error when an Inverse Distance Weighted (IDW) method was applied. Therefore, the total RMS error of the DEM was 19 m. The coverage of this DEM was not successful in some sectors where the aerial photographs used by the IGM in the restitution process exhibited stereo matching problems due to snow covered surfaces, steep flanks or shadows slopes.

Shuttle Radar Topography Mission (SRTM) data obtained from JPL/NASA in 2000 were also collected covering the majority of the study area, with the exception of small sections that lacked topographic information due to their rough topography and steep slopes. At the margins of these non-data areas some spurious pixels were identified

with altitude values more than 50 m lower than the surrounding pixels. These incorrect elevations are a consequence of the conversion applied by JPL/NASA when reducing the original 30 m pixel size to the 90 m resolution available in the public domain. These spurious pixels were manually detected and eliminated, following a similar procedure to Rignot et al. (2003).

In order to estimate SRTM vertical errors, rock areas were compared between both DEMs yielding a small bias (1.8 m) and a vertical random error of 20.9 m (one standard deviation). This vertical random error is composed of the inaccuracies of the IGM DEM (19 m) and the error of SRTM (9 m), including a possible bias between SRTM and altitude (Berthier et al., 2006). These errors are similar to the

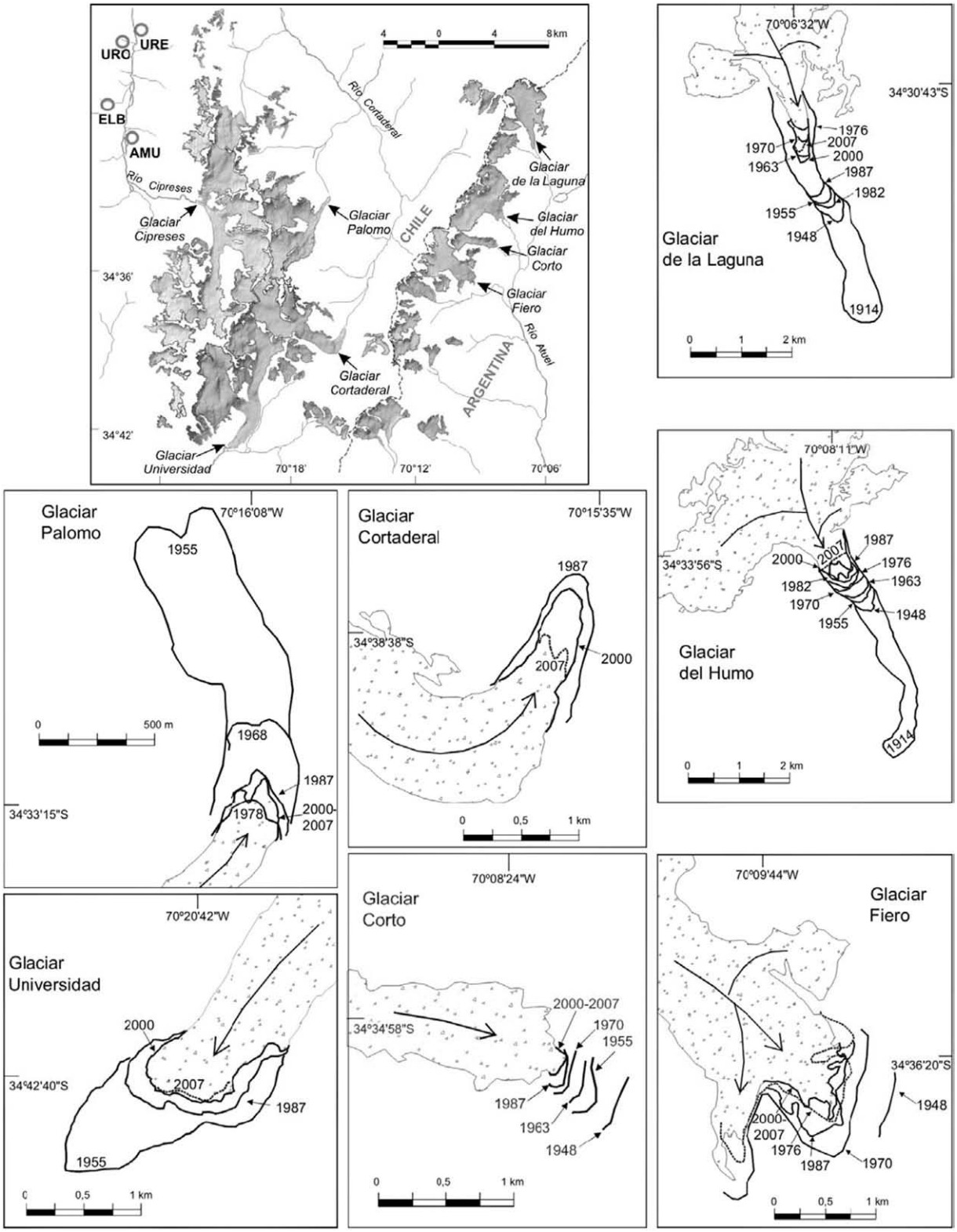

Fig. 3. The upper left panel shows the location of the main glacier areas (year 2000) and the *Austrocedrus chilensis* tree-ring chronology sites (circles). See Table 3 for details of each site. Individual panels show the fluctuations in frontal positions of the main glaciers in the study area. Arrows indicate the main ice flow directions.

Table 3
Site and characteristics of *Austrocedrus chilensis* tree-ring chronologies.

Site name and code	Lat S–Long W	Elevation (m)	Time span (yr)	Number of series	Mean series length (yr)
El Asiento (ASI)	32°29′–70°49′	1700–1900	955–2000	117	298
El Baule-Urriola (ELU)*	34°27′–70°26′	1600–1900	1149–2001	143	340
Agua de la Muerte (AMU)	34°31′–70°25′	1700–2000	1072–2001	107	368

*Composite chronology.

results obtained in Patagonia by Rignot et al. (2003), after comparing SRTM and DEMs derived from the IGM regular cartography.

2.3. Dendrochronological records

Austrocedrus chilensis tree-rings are well defined (Roig, 1992) and highly sensitive to moisture variability. During the last decades, this conifer has been extensively used as a precipitation proxy in the south-central Andes of Argentina and Chile (Boninsegna, 1992; Villalba et al., 1998; Le Quesne et al., 2006).

The trees sampled for this study were found near the northern limit of the natural distribution area of the species (Fig. 1), at 32°39′ S in El Asiento (some 80 km north of Santiago) and at 34°40′S in Río Cipreses Valley (100 km south of Santiago). The trees grow in very steep rocky environments between 1600 and 2200 m altitude, where they are subject to moisture stress during the dry summer season (Fig. 2). The arid and relatively cold habitat favours good preservation of subfossil wood, which was used to extend the chronologies back in time. Some of the *A. chilensis* sites that yielded chronologies in early collections (LaMarche et al., 1979) were revisited and updated with new collections. Other sites were added to develop a chronology network on Río Cipreses Valley (Figs. 1 and 3), with some specimens older than nine hundred years (Le Quesne et al., 2006). The network used for this study includes; El Asiento (ASI) chronology from the northern limit of the species (LaMarche et al., 1979); a composite chronology (ELU, Table 3) of three sub-sampled sites (East Urriola-URE, West Urriola-URO and El Baule-ELB; Fig. 3) located in the lower portion of the Cipreses valley; and a chronology in Agua de la Muerte (AMU) from the upper portion of the valley, only 5 km from the present frontal terminus of Glaciar Cipreses (Table 3; Figs. 1 and 3).

Core samples were prepared following standard dendrochronological techniques (Schweingruber et al., 1990; Stokes and Smiley, 1996). Ring widths were measured using an incremental measuring machine at 0.01 mm precision level. The ring width series were visually cross-dated and then, the accuracy of the dating process tested using the COFECHA programme (Holmes, 1983).

The cross-dated samples were standardised using the regional curve method (Briffa et al., 1992) in order to remove the biological growth trend, while retaining the low frequencies related to climate. The standard chronologies were generated using ARSTAN program (Cook and Holmes, 1984).

2.4. Precipitation reconstruction

Santiago de Chile has a continuous record of monthly mean precipitation beginning in 1866. The station is located in Quinta Normal (33°26′ S; 70°41′ W, 520 m asl) where it is controlled by the Dirección Meteorológica de Chile (DMC), and provides the longest and most reliable record in the area.

The growth of *A. chilensis* shows significant positive correlation with the monthly mean Santiago de Chile precipitation from April to November (Boninsegna, 1988; Le Quesne et al., 2006). Although the May–November period accounts for ca. 80% of the total annual

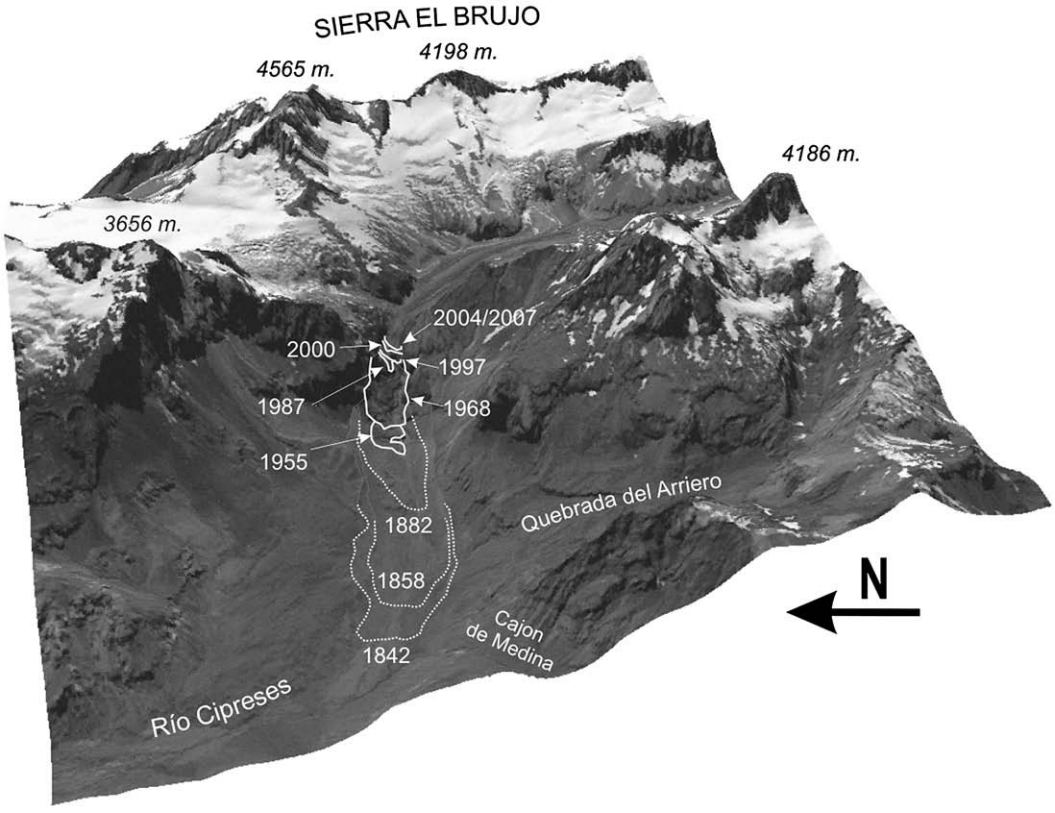

Fig. 4. Landsat ETM+ panchromatic image acquired on January 20, 2000, superimposed on SRTM data. Glaciar Cipreses frontal positions reconstructed from historical documents (dotted lines), aerial photographs and satellite images (solid lines) are indicated.

precipitation, the total annual precipitation was used, in order to better capture the inter-annual precipitation variability. As the relationship between tree-ring indices and annual precipitation is not linear; a lineal model was fitted to the instrumental precipitation through natural logarithmic transformation.

A tree-ring based multivariate model was developed to reconstruct Santiago precipitation between 1866 and 1999, using the three standard tree-ring chronologies as predictors (Table 3). In the multi-regression model the three chronologies were incorporated at year t and lagged at year $t-1$ and $t+1$, because the radial growth of trees is influenced by climatic conditions during the current and in the following year through complex physiological processes affecting buds, leaf growth, and reserve accumulation. Due to this relationship, the ring width at the year $t-1$ is statistically related to the ring width of the year t and is included in the model to account for autocorrelation (Fritts, 1976). Therefore, the chronologies in year $t-1$, t and $t+1$ were used as candidate predictors of year t precipitation (e.g., D'Arrigo and Jacoby, 1991; Villalba et al., 1997).

In order to avoid co-linearity, principal components were extracted from the nine candidate tree-ring predictor variables and the factor scores were used to replace the original variables of the time series (Villalba et al., 1998; Bradley, 1999). To select the best subset regression models, the maximum adjusted r-squared criterion (Adj R^2) was used (Draper and Smith, 1981). The reconstruction models were tested by dividing instrumental precipitation (1866–1999) into early and late sub-periods to perform the calibration–verification exercises (e.g., Fritts, 1976; Cook and Kairiukstis, 1990).

2.5. Spectral methods

Two spectral methods were used to detect non-stationary oscillatory modes of variability in the 712-yr series of reconstructed precipitation. Firstly, the distribution of the variance and the signals contained in the reconstruction were examined using Continuous Wavelet Transform (CWT) analysis (Torrence and Compo, 1998). CWT analysis allows the detection of periodic significant signals (waveforms) by expanding one-dimensional time series into two-dimensional time-frequency space (Grinsted et al., 2004). This method allowed the simultaneous representation of the dominant modes of variability (periodic signals) and the variation of those modes in time (Torrence and Compo, 1998). The CWT analysis was conducted using the Matlab routine WTC-R15 provided by Grinsted et al. (2004). Secondly, the periodic behaviour of the reconstructed time series was evaluated by extracting the dominant (i.e., eigenvalue>1) oscillatory components (wave forms) using Singular Spectral Analysis (SSA; Vautard and Ghil, 1989). The dominant wave forms of the reconstruction were combined into secular, decadal/inter-decadal, and inter-annual timescale periods, in order to facilitate the comparison with glacier variations. The Singular Spectral Analysis was performed by using the SSA programme (Boninsegna and Holmes, unpublished operating manual [Laboratory of Tree-Ring Research, University of Arizona]).

3. Results

3.1. Glacial variations

Glaciar Cipreses is one of the few glaciers in the study area with a century-long historical record. This glacier has been frequently visited by naturalists since 1831 when the first record was obtained by Claudio Gay who documented moraines and described erratic blocks at the front of the glacier. Since then, several accounts (summarized in Fig. 4 and Table 4) were obtained from Pissis (1860), Espejo (1897), Barros Arana (1911), Risopatrón (1924) and Domeyko (1978). The only interruption to the retreat trend of Glaciar Cipreses during the19th century took place in 1858, when a re-advance of the glacier was reported by Pissis (1875) and also documented by Röthlisberger (1986). Concurrently, an advance was registered for Glaciar Los Piuquenes (34°22′S 70°04′W), located 30 km to the northeast of Glaciar Cipreses (Plagemann, 1887). In 1882, Glaciar Cipreses was again under a severe retreat trend, as illustrated by a large mass of ice located 1.5 km downstream from the glacier tongue (Güssfeldt, 1884). Unfortunately, no historical records were collected between 1882 and 1955, with the exception of the visit of Nogues (1894). Since 1955, the glacier retreat has been documented thanks to several aerial photographs and satellite images (Table 3).

Table 4
Frontal variations of studied glaciers in the Central Andes.

Glacier name	Country	Period	Length change (m)	Annual length change (m y^{-1})	Source
Cipreses	Chile	1842–1852	−377	−38	a
		1852–1882	−1730	−58	a
		1882–1955	−977	−13	b
		1955–1968	−428	−33	b
		1968–1987	−796	−41	b
		1987–1997	−58	−6	b
		1997–2000	−66	−23	b
		2000–2004	−52	−12	a
		2004–2007	0	0	a
Total		1842–2007	−4484	−27	
Universidad	Chile	1945–1955	−1000	−100	c
		1955–1987	−778	−24	a
		1987–1997	−57	−6	a
		1997–2000	−130	−45	a
		2000–2007	−35	−5	a
Total		1955–2007	−1000	−19	
Cortaderal	Chile	1987–2000	−110	−9	a
		2000–2007	−460	−66	a
Total		1987–2007	−570	−29	
Palomo	Chile	1955–1968	−910	−71	d
		1968–1978	−250	−25	d
		1978–1987	88	10	a
		1987–2000	−31	−2	a
		2000–2007	0	0	a
Total		1955–2007	−1103	−21	
de la Laguna	Argentina	1914–1948	−2200	−65	e
		1948–1955	−440	−63	e
		1955–1963	−1000	−125	e
		1963–1970	−300	−43	e
		1970–1982	1400	117	e
		1982–1987	−350	−67	a
		1987–2000	−703	−55	a
		2000–2007	−220	−31	a
Total		1914–2007	−3813	−41	
Humo	Argentina	1914–1948	−3200	−94	e
		1948–1955	−300	−43	e
		1955–1963	−160	−20	e
		1963–1970	−300	−43	e
		1970–1982	−150	−12	e
		1982–1987	−103	−20	a
		1987–2000	−164	−13	a
		2000–2007	−250	−36	a
Total		1914–2007	−4627	−50	
Corto	Argentina	1948–1955	−188	−27	e
		1955–1963	−90	−11	e
		1963–1970	−99	−14	e
		1970–1987	−34	−2	a
		1987–2000	−54	−4	a
		2000–2007	0	0	a
Total		1948–2007	−465	−8	
Fiero	Argentina	1948–1955	−12	−2	e
		1955–1963	−80	−10	e
		1963–1970	−300	−43	e
		1970–1987	89	5	a
		1987–2000	−224	−17	a
		2000–2007	0	0	a
Total		1948–2007	−527	−9	

[a]This work; [b]Rivera et al. (2000); [c]Lliboutry (1956); [d]Caviedes (1979); [e]Cobos and Boninsegna (1983).

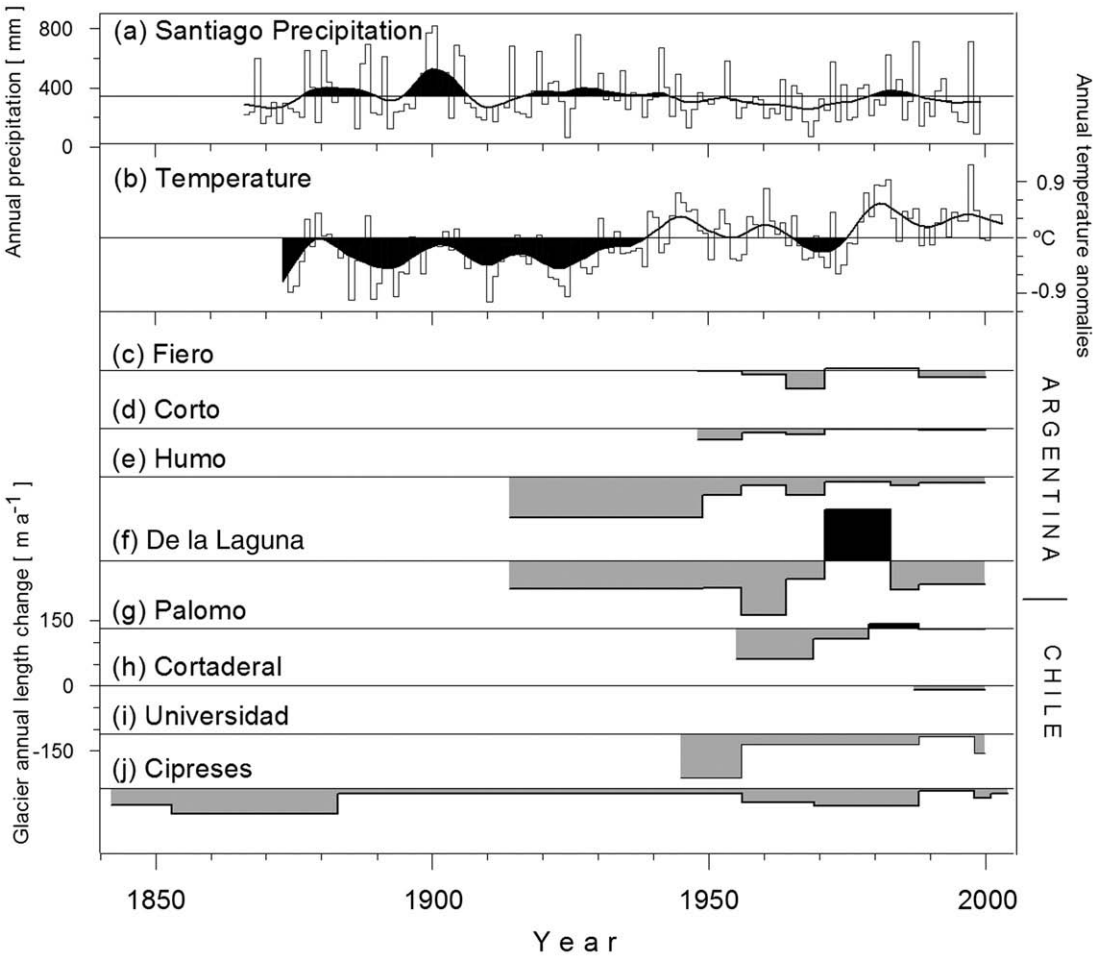

Fig. 5. (a) Santiago de Chile annual precipitation (1866–1999) from Dirección Meteorológica de Chile (DMC). (b) Annual mean temperature data (1873–2003) for Central Chile (30–35°S, 70–75°W) acquired from the land and marine grid-box (5°×5°) temperature anomaly dataset (Jones and Moberg, 2003). Both series were fitted with a 15-yr smoothing spline to highlight decadal variability. Annual length change for the eight studied glaciers in the Andes of Argentina (c–f) and Chile (g–j).

Other glaciers in the study area have followed a similar trend, with generalized retreats since the beginning of the 20th century and in some cases since the first remotely sensed imagery were collected in the 1950s (Table 4, Figs. 3 and 5). In spite of the overall receding trend, several glaciers experienced advances during the 1970s and 1980s, for example, Glaciar de la Laguna, which advanced 1400 m between 1970 and 1982 (Figs. 3 and 5) in what is considered a surging event (Cobos and Boninsegna, 1983). Since then however, all glaciers have been retreating, with significant area losses up to the year 2007 (Table 5).

After comparing DEMs from 1955 and 2000 for the main glaciers on the Chilean side of the Andes, significant changes were documented in Glaciar Cipreses, Palomo and Universidad, which have experienced ice elevation changes of −0.76, −0.6 and -0.56 ± 0.47 m y^{-1} (SRTM-IGM DEM) respectively.

3.2. Tree-ring precipitation reconstruction

For this study, 367 tree-ring samples from dead and living trees of long-lived coniferous *A. chilensis* were combined to develop a robust network of moisture-sensitive tree-ring data (Table 3). The network comprises tree-ring series ranging from 1200 to 150 yr, with a mean segment-length of ca. 335 yr. The chronologies ASI, ELU and AMU, include 42, 51 and 58% of the samples >300 yr, respectively. This feature, along with the appropriate sample replication and the conservative standardization method (RCS) used to maximize the climatic signal, assumes that the dendrochronological record captures an appreciable amount of both low and high frequencies in precipitation variability.

The results of the calibration–verification experiments using PC factor scores of tree-ring chronologies as predictors of annual precipitation are summarized in Table 6. The number of orthogonal tree-ring variables entered into the regression models was 5. Cross-validation tests were performed from the 1866 to 1999 interval (full period). The observed precipitation time series was split into two sub-periods, using the earlier part of the record (1866–1933) for calibration and the later part (1934–1999) as independent verification of tree-rings estimates of precipitation. Subsequently, the same calibration–verification procedure was applied with reversed sub-periods. Pearson coefficient results (0.71, 0.76) are indicators of the reconstruction validity. The RE statistic (>0.5) is a measure of shared variance between the actual and modelled series, and any positive value denotes that the regression model provides valuable palaeoclimatic information (for further details in calibration and verification see Cook and Kairiukstis, 1990).

The regression model for annual precipitation accounts for 52% of the total variance over the full calibration interval (134 yr). Although the relationship for the entire calibration interval is not as good as for the earliest sub-period, the full record was used in order to enhance the ability of the model to capture the long-term precipitation variability (Table 6). The observed precipitation with the tree-ring reconstructed precipitation is shown in Fig. 6. As previously noted by Boninsegna (1988), *A. chilensis* tree-rings are better at estimating extreme dry- than extreme wet-years such as 1877, 1880, 1888, 1899–

Table 5
Areal changes of some Central Andes glaciers.

Glacier Name	Country	Period	Frontal areal change	Rate
			km^2	$km^2\ yr^{-1}$
Cipreses	Chile	1842–1852	−0.63	−0.063
		1852–1882	−1.53	−0.051
		1882–1955	−0.78	−0.011
		1955–1968	−0.14	−0.011
		1968–1987	−0.35	−0.019
		1987–1997	−0.01	−0.001
		1997–2000	−0.02	−0.007
		2000–2004	−0.01	−0.004
Total		1842–2004	−3.48	−0.022
Universidad	Chile	1955–1987	−0.74	−0.023
		1987–2000	−0.25	−0.019
		1955–2000	−0.99	−0.022
Cortaderal	Chile	1987–2000	−0.25	−0.019
Palomo	Chile	1955–1968	−0.35	−0.027
		1968–1978	−0.12	−0.012
		1978–1987	0.03	0.003
		1987–2000	−0.01	−0.001
Total		1955–2000	−0.45	−0.01
de la Laguna	Argentina	1914–1948	−1.28	−0.038
		1948–1955	−0.19	−0.027
		1955–1963	−0.33	−0.041
		1963–1970	−0.08	−0.011
		1970–1976	−0.06	−0.009
		1976–1982	0.57	0.095
		1982–1987	−0.13	−0.026
		1987–2000	−0.23	−0.018
Total		1914–2000	−1.72	−0.02
Humo	Argentina	1914–1948	−1.15	−0.034
		1948–1955	−0.09	−0.013
		1955–1963	−0.06	−0.007
		1963–1970	−0.12	−0.017
		1970–1976	−0.06	−0.01
		1976–1982	−0.07	−0.011
		1982–1987	−0.06	−0.012
		1987–2000	−0.09	−0.007
Total		1914–2000	−1.7	−0.02

1900, 1914, 1926, 1941, 1982, 1987 and 1997, the ten wettest years in the instrumental precipitation series of Santiago since 1866 (Fig. 6). Tree-rings typically underestimate wet extremes, because soil properties and tree physiology limit the response of tree growth to abundant precipitation (Meko et al., 1995; Villalba et al., 1998).

Using the model derived in the calibration, the precipitation was reconstructed back to AD 1280. The entire precipitation reconstruction is showed in Fig. 7a (top panel), along with a 25-yr smoothing spline (Cook and Peters, 1981), to highlight long periods of above and below-mean precipitation.

The second panel of Fig. 7 shows the wavelet power spectrum (CWT) of the precipitation, displayed as a function of the period and time. At the beginning and the end of the time series, the edge effect (defined by the cone of influence) becomes relevant, and consequently the results should be interpreted cautiously (Torrence and Compo, 1998).

In general, the results of the long-term reconstructed precipitation variability show that the amplitudes and relative power of the detected signals changes substantially over time (Fig. 7b). The wavelet analysis shows a significant contribution of the variance in the inter-annual and decadal/inter-decadal (<23 yr periods) frequency band. This is shown by the oscillatory modes extracted with SSA and grouped in 2.1–3.4 (Fig. 7e) and 13–23 yr (Fig. 7d), which explain ca. 37% of the total variance. At lower frequencies a secular trend (Fig. 7b) delineated at the bottom of the Cone of influence (>100 yr) contribute with ca. 11%. The long-term multidecadal waves around 35 and 85–93 yr are not detected by SSA, because they account for only 0.9% and 3% of the total variance.

The secular trend (208-yr waveform) extracted by SSA (Fig. 7c), explains 11.6% of the variance and captures the long-lasting dry and wet periods over the last seven centuries. Note the decline since the late 19th century (ca. 1890) to the present, and the prolonged dry spells during early 18th (1700–1735), late 16th and early 17th (1570–1635), and the majority of the 14th to the first half of 15th (1330–1450) centuries. Wet conditions occur with maxima centred on the years AD 1500, 1650 and 1850.

Decadal/inter-decadal modes (13.0–23.0 yr; Fig. 7d), explain 18.5% of the variance, and are characterised by several multiyear periods of reduced amplitudes over the 700-yr long reconstruction. To mention the most noticeable episodes: early to mid 20th (1915–1970), mid 17th to mid 18th (1660–1740), 16th and first half of 17th (1500–1570 and 1595–1640) and mid 14th to mid 15th (1350–1440) centuries. Enhanced decadal variability took place during the following periods: AD1890–1910, 1740–1770, 1640–1660, 1570–1595 and 1445–1500.

The inter-annual oscillatory mode (2.1–3.4 yr; Fig. 7e), which explains 18.4% of the variance, is characterised by several periods of both reduced and increased variability. Within the episodes of lesser variability, the ca. 150-yr long period (1700–1850) is interrupted by a peak of variance that occurs in the late 19th century. Other periods of increased and decreased inter-annual variability include the late 16th to early 17th centuries (1590–1605) and the majority of the 15th century (1410–1490), respectively.

The comparison of inter-annual and decadal modes (Fig. 7d–e) with the El Niño 3.4 SST (Hurrell et al., 2008) and PDO index (not shown here), reveals a strong relation with tropical Pacific conditions contrasting with a weak relationship with the PDO (Mantua et al., 1997). The N3.4 inter-annual signal (2.0–3.6 yr) extracted by SSA correlates at $r=0.36$ (for the common period 1871–1993), whilst the PDO index reaches only an $r=0.22$ (for the common period 1900–1993). Interestingly, the decadal signal (13.0–22.0 yr) extracted from N3.4 series correlates with $r=0.44$ for the common period 1871–1993, and with $r=0.69$ from 1886 to 1993 (Fig. 7d).

4. Discussion

Several sources have documented the widespread retreat of glaciers in the Central Andes during the 19th and 20th century (Cobos and Boninsegna, 1983; Rivera et al., 2000; Luckman and Villalba, 2001). The historical record from Glaciar Cipreses, shows the same trend observed in both slopes of the Andes during the 19th century (Philippi 1867; Güssfeldt 1883; Hauthal 1895, Martin 1909). In spite of the longer record, no information is available for Glaciar Cipreses between the end of the 19th century to 1955 (Table 4; Fig. 4) thus exhibiting a hiatus in the historical record. The reconstructed period of glacier fluctuations is particularly important as it coincides with decades of relatively high (1880 to 1910) and low precipitation (1950 to 1970; Figs. 5 and 6), when several glaciers in the Mendoza (Luckman and Villalba, 2001) and Chilean (Lliboutry, 1956) Andes experienced advances and retreats, respectively.

The tree-ring chronologies obtained here allowed reconstruction of 700 yr of precipitation variability in Santiago of Chile. This is the longest and most reliable record ever obtained for Santiago, where the inter-annual and decadal/inter-decadal variability explains up to 37% of the variance. The centennial trend contributes to 11% of the variance. In the

Table 6
Calibration and verification statistics for the tree-ring-based Santiago de Chile precipitation reconstruction.

Time period	Calibration		Verification	
	Adj R^2	n	r	RE
1866–1933	0.58	5	0.71	0.49
1934–1999	0.50	5	0.76	0.59
1866–1999	0.52	5		

Adj R^2 is the variance explained accounting for the loss of degrees of freedom, n; number of predictors used in the regression analyses; r, the Pearson correlation coefficient; RE, reduction of error statistic, this statistic ranges from $-\infty$ to $+1$ and any positive value indicate that the reconstruction provides unique palaeoclimatic information.

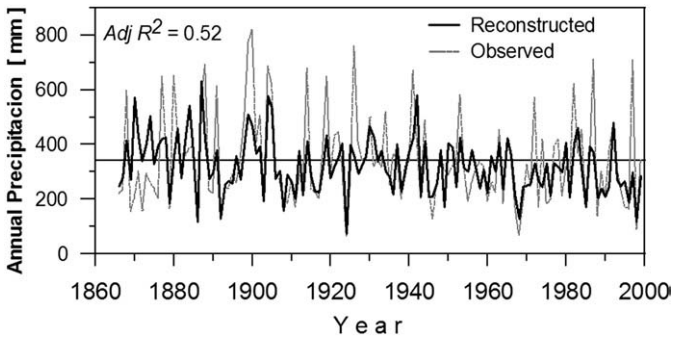

Fig. 6. The instrumental and reconstructed Santiago de Chile annual precipitation for the interval 1866 to 1999. The calibration was based on the natural-log transformed version of the instrumental precipitation series.

700-yr series, a non-stationary mode of variability was found, with periods of prevalent decadal oscillations (e.g., 1450 to 1500 AD). Conversely in other periods the inter-annual variability dominates (e.g., 1670–1700 AD). At the beginning and end of the time series (i.e., before 1430 AD and after 1900 AD), the centennial wave is indicating noticeable drought conditions. In between, three peaks of wetter conditions are clearly visible around years 1500, 1650 and 1850 AD. Precipitation is reconstructed to have decreased from this last maximum in precipitation to the present. This trend is coincident with the instrumental (Quintana, 2004) and previously reconstructed precipitation (Boninsegna, 1988) records, with increasing risk of drought conditions in Central Chile (Le Quesne et al., 2006), upward migration of the snowline (Carrasco et al., 2005), and generalised glacier retreats (Rivera et al., 2002). Therefore, the *Austrocedrus* tree-ring chronologies utilised here must be considered a valid proxy for precipitation reconstructions, confirming previous studies by Boninsegna (1988) and Luckman and Villalba (2001).

Unfortunately, temperature response of these trees is relatively weak and confined to the spring season (Le Quesne et al., 2000). Therefore, only instrumental temperature records have been considered for the analysis. For this purpose, we used the annual mean temperature data (°C 1873–2003) for Central Chile (30–35°S, 70–

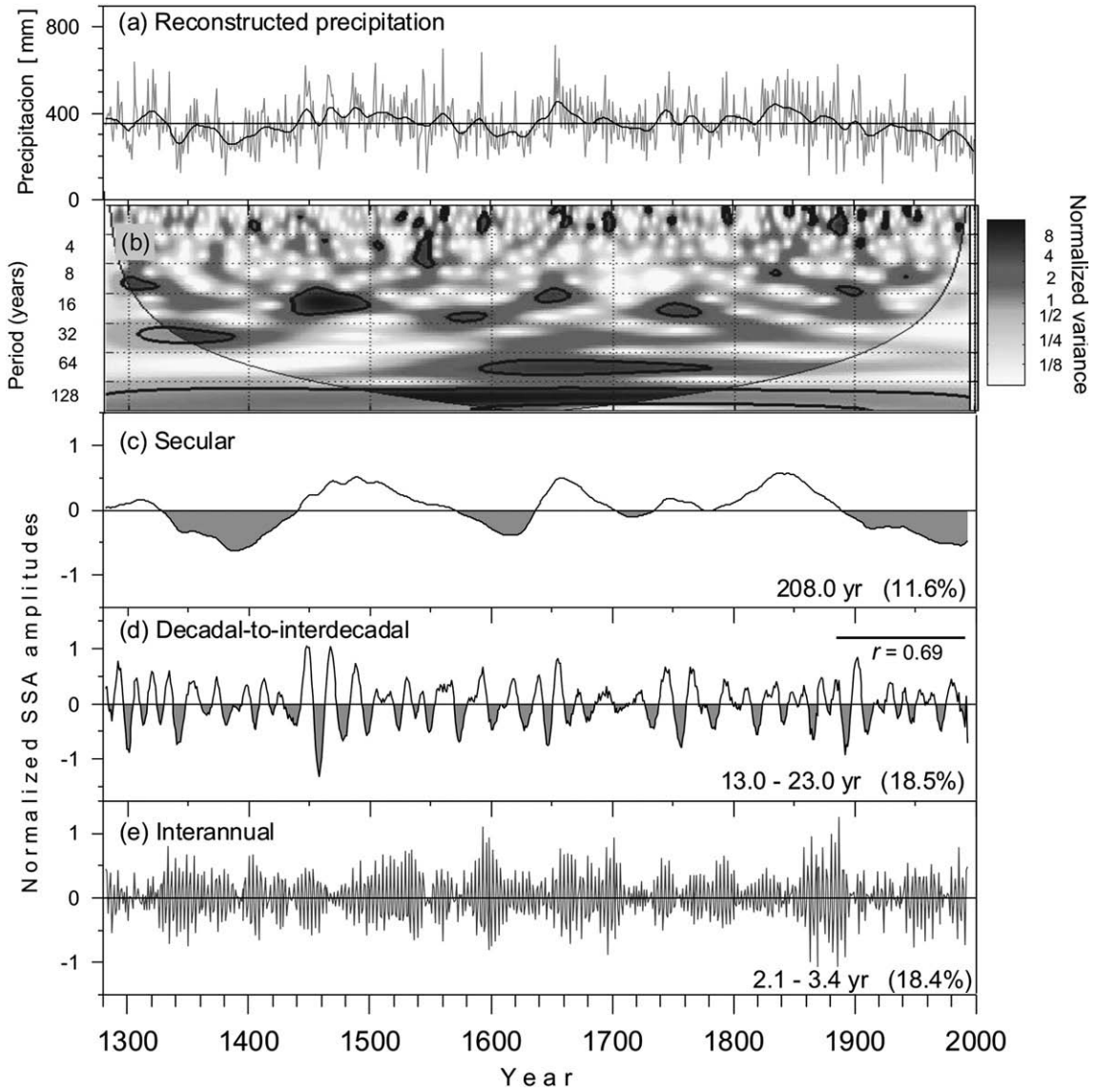

Fig. 7. (a) The tree-ring reconstruction of Santiago de Chile precipitation from AD 1280–1999. A 25-yr smoothing spline highlights the decadal variability. (b) Continuous Wavelet Transform (CWT) was used to identify the dominant modes of variability (or periodic signals in the reconstructed precipitation) at different time scales. The left axis is the Fourier period and the bottom axis represents the time in years. The grey gradient represents the percentage (%) of the wavelet power and the thick black contour demarcates significant modes of variance at 95% against the red noise. Within the cone of influence, shown as a lighter shade, edge effects become important. (c–e) Secular, decadal/inter-decadal and inter-annual signals extracted by Singular Spectral Analysis (SSA) with the corresponding explained variance in percentage (%). In (d), the interval of comparison ($r = 0.69$) between decadal oscillations in the N3.4 series (13–22 yr) and the reconstruction (13–23 yr) are indicated.

75°W) acquired from land and marine temperature grid cells (Jones and Moberg, 2003) (Fig. 5b). This series shows a long-term increase in temperature, with two clear jumps in 1947 and the 1970s, the latter coincident with the well-known PDO shifts (Giese et al., 2002). The first part of the series (before the 1940s) is characterised by a semi permanent cold anomaly followed by warmer conditions during the 1950s. During the period of frequent La Niña years in the 1960s and 1970s, temperature decreased, reaching a minimum just before 1976. After the PDO shift in 1976, temperature rapidly increased, and has remained relatively stable in the last quarter of 20th century.

The Central Chilean and Argentinean glaciers are part of the complex, mountain systems, directly affected by changes in temperature and precipitation, and subsequently, snow variability. The response of the glaciers and trees to these climatic variables is not immediate, with lag times varying from years to several decades in the case of glaciers (Paterson, 1994), and from seasons to years in the case of *Austrocedrus* (Fritts, 1976). In both cases, years with above (below) mean precipitation result in wider (thinner) *Austrocedrus* ring widths and positive (negative) glacier mass balances. Additionally, lower (higher) than normal spring temperature values cause wider (thinner) tree-ring widths and positive (negative) glacial mass balances. Although modern glaciers and trees from this region exhibit similar responses to variations in precipitation and temperature during historical times, the interactions between the climate, trees and glaciers in central Chile and Argentina are not always straightforward.

Little is known about glacial behaviour during pre-historical times; with the exception of some moraine dating conducted in the region (Röthlisberger, 1986; Villalba, 1994; Espizúa, 2003). Thus, we speculate that glaciers were following climatic trends as illustrated in our reconstruction. Based on above-mean precipitation, ca. 1450, 1650 and 1850 AD, glaciers were most likely advancing during these intervals. However, the only glaciological data we have to support this suggestion is the reported advance of Glaciar Cipreses in the mid 1850s, presumably in response to the extended last wet period in the reconstruction.

The high variance of the reconstructed precipitations (ca. 18%), as explained by the ENSO related frequencies (2.1–3.4 yr), is a result of the documented sensitivity of central Chile climate to the equatorial Pacific conditions (Escobar and Aceituno, 1998; Montecinos and Aceituno, 2003; Garreaud et al., 2009-this issue). However, the results obtained here suggest that this climatic forcing can also modulate the precipitation variability at lower frequencies (13.0–23 yr; i.e., decadal/inter-decadal scale). This means that decadal/inter-decadal warm (cold) sea surface conditions are associated with warm (cold) and wet (dry) climate conditions in the study area, similar to the inter-annual phenomenon El Niño and La Niña (see also Barichivich et al., 2009-this issue).

5. Conclusions

All glaciers have a net retreat between 1955 and 2007, with mean frontal rates of -22 m yr^{-1} and -15 m yr^{-1}in the Chilean and Argentinean sides of the Andes, respectively. If we consider the historical data obtained for Glaciar Cipreses between 1842 and 1955, the frontal retreat of ca. 4.5 km resulted in a total area loss of approximately 3.5 km^2. Ice elevation changes measured in several glaciers also confirm the shrinking trend within the ablation areas, with thinning rates between -0.76 and -0.56 ± 0.47 m yr^{-1} between 1955 and 2000. On average, the glaciers of the study area in year 2000 were approximately 3% smaller than in 1955. This surface loss occurred in both sides of the Andes and was observed mainly at the ablation areas.

All these changes in glacier area are predominantly driven by the combination of the atmospheric warming, as illustrated by the increase in altitude of the 0 °C degrees isotherm, and the secular reduction in precipitation, namely during the last 150 yr as inferred from the reconstructed series. Atmospheric temperatures in Central Chile and Argentina have experienced two distinctive positive shifts since the beginning of instrumental records in mid 19th century (ca. 1940s and 1970s), the latter in agreement with the Pacific Decadal Oscillation shift widely described in the climatological literature.

The glacial retreat has been interrupted by two minor periods of advance (mid 1850s and mid 1980s), however, the lack of glaciological data from the beginning of the 20th century is most likely obscuring a third advancing cycle, which has been registered in glaciers located further north (Lliboutry, 1956).

From the wet period observed in the last two decades of the 19th century, the reconstructed precipitation of Santiago shows a negative trend during most of the 20th century (Aceituno et al., 1993; Luckman and Villalba, 2001; Quintana, 2004). Both, the instrumental record and the reconstructed precipitation indicate that the 19th century was wetter than the 20th. This is coincident with Central Chile rainfall reconstructions derived from different methods (Le Quesne et al., 2006).

The trees used in this study are located at relative long distances from the glacier. Due to the extreme scarcity of organic matter in the upper mountain regions in Central Chile, it is not possible to use ^{14}C to date the moraines, as is common in many sites in Patagonia (Villalba et al., 1990). In order to overcome this problem, it is recommended that future studies of glacier variations in Central Chile utilize a multi-proxy approach, including several proxies such as historical documents, lake sediments, and lichenometry.

Acknowledgements

This research was funded by a CONICYT-Chile project FONDECYT 3020011; the Inter American Institute for Global Change Research grant CRN03 (Americas Treeline Environment) and CECS. CLQ thanks the Millennium Nucleus P01-051-F, Universidad Austral de Chile, for a postdoctoral fellowship. We are grateful to D. Shea from the NCAR Climate and Global Dynamics Division for the N3.4 SST record compiled from Hurrell et al. (2008). CONAF (in particular Julio Cesar Vergara and Joaquín Bruna) provided valuable field-work support. María Eugenia Solari collaborated with the searching of historical documents. CECS is funded by the Base Financing Program of CONICYT-Chile and the Millennium Science Initiative. Comments from Mathias Vuille, Neil Glasser and Ricardo Villalba are highly appreciated. We thank Louise Newman, PAGES Office, for improving the English style.

References

Aceituno, P., Fuenzalida, H., Rosenblüth, B., 1993. Climate along the extratropical west coast of South America. In: Mooney, H.A., Fuentes, E.R., Kronberg, B.I. (Eds.), Earth System Responses to Global Change: Contrast between North and South America. Academic Press, New York, pp. 61–69.

Barichivich, J., Sauchyn, D.J., Lara, A. 2009. Climate signals in high elevation tree-rings from the semiarid Andes of north-central Chile: responses to regional and large-scale variability. Palaeogeogr. Palaeoclimatol. Palaeoecol. 281, 320–333 (this issue).

Barros Arana, D., 1911. Don Claudio Gay, su vida y sus obras. Capítulo II Antecedentes Biográficos de Gay- su primer viaje a Chile. Obras Completas de Diego Barros Arana Tomo XI, Estudios Histórico-Bibliográficos. Imprenta Cervantes, Santiago.

Berthier, E., Arnaud, Y., Vincent, C., Remy, F., 2006. Biases of SRTM in high-mountain areas: implications for the monitoring of glacier volume changes. Geophys. Res. Lett. 33 (8), L08502. doi:10.1029/2006GL025862.

Boninsegna, J.A., 1988. Santiago de Chile winter rainfall since 1220 as being reconstructed by tree rings. Quat. South Am. Antarct. Penins. 6, 67–87.

Boninsegna, J.A., 1992. South American dendrochronological records. In: Bradley, R.S., Jones, P.D. (Eds.), Climate Since A.D. 1500, Routledge, Chapman and Hall, London and New York, pp. 446–462.

Bradley, R.S., 1999. Paleoclimatology: Reconstructing Climates of the Quaternary, Second Edition. Academic Press, San Diego.

Bradley, R.S., Briffa, K.R., Cole, J., Hughes, M.K., Osborn, T.J., 2004. The climate of the last millennium. In: Steffen, W. (Ed.), Global Change and the Earth System, a Planet Under Pressure. The IGBP Series. Springer Verlag, Berlin, pp. 105–149.
Briffa, K.R., Jones, P.D., Bartholin, T.S., Eckstein, D., Karlén, W., Zetterberg, P., Eronen, M., 1992. Fennoscandian summers from AD 500: temperature changes on short and long timescales. Clim. Dynam. 7, 111–119.
Bruce, R., Cabrera, G., Leiva, J., Lenzano, L., 1987. The 1985 surge and ice dam of Glaciar Grande del Nevado del Plomo, Argentina. J. Glaciol. 33 (113), 131–132.
Carrasco, J.C., Quintana, J., Casassa, G., 2005. Changes of the 0 °C isotherm and the equilibrium line altitude in central Chile during the last quarter of the 20th century. Hydrol. Sci. J. 50 (6), 933–948.
Caviedes, J., 1979. Inventario de glaciares en la hoya del río Cachapoal y predicción de la escorrentía de deshielo; Andes Centrales. Memoria, Escuela de Geología, Universidad de Chile. 217 pp.
Cobos, D.R., Boninsegna, J.A., 1983. Fluctuations of some glaciers in the upper Atuel River basin, Mendoza, Argentina. Quat. South Am. Antarct. Penins. 1, 61–82.
Cook, E.R., Holmes, R.L., 1984. Program ARSTAN User Manual. Laboratory of Tree-Ring Research, University of Arizona, Tucson.
Cook, E.R., Kairiukstis, L.A., 1990. Methods of Dendrochronology: Applications in the Environmental Science. Kluwer Academic Publishers, Dordrecht.
Cook, E.R., Peters, K., 1981. The smoothing spline: a new approach standardizing forest interior tree-ring series for dendroclimatic studies. Tree-Ring Bull. 41, 45–53.
D'Arrigo, R.D., Jacoby, G.C., 1991. A 1000-year record of winter precipitation from northwestern New Mexico, USA: a reconstruction from tree-rings and its relation to El Niño and the Southern Oscillation. Holocene 1, 95–101.
Domeyko, I., 1978. Mis viajes Memorias de un exiliado, Tomo I. Ediciones Universidad de Chile, Santiago. (original in Polish University of Cracovia 1962).
Draper, N.R., Smith, H., 1981. Applied Regression Analysis, 2d ed. John Wiley & Sons, NY.
Escobar, F., Aceituno, P., 1998. Influencia del fenómeno ENSO sobre la precipitación nival en el sector andino de Chile central durante el invierno. Bull. Inst. fr. études Andines 27, 753–759.
Espejo, P., 1897. Baños de Cauquenes Guía del Bañista i del Turista, Santiago.
Espizúa, L., 1993. Quaternary glaciations in the Río Mendoza Valley, Argentine Andes. Quat. Res. 40, 150–162.
Espizúa, L., 2003. Holocene glacier fluctuations in the south of Mendoza Andes, Argentina. Actas II Congreso Argentino de Cuaternario y Geomorfología, Tucumán, vol. 1, pp. 87–92.
Falkner, E., 1995. Aerial mapping. Methods and Applications. CRC Press Inc, USA.
Fritts, H.C., 1976. Tree Rings and Climate. Academic Press, London.
Garreaud, R., Vuille, M., Compagnucci, R., Marengo, J. 2009. Present-day South American climate. Palaeogeogr. Palaeoclimatol. Palaeoecol. 281, 180–195 (this issue).
Giese, B., Urizar, C., Fuckar, N., 2002. Southern hemisphere origins of the 1976 climate shift. Geophys. Res. Lett. 29 (2) 10.1029-2001GL013268.
Grinsted, A., Moore, J.C., Jevrejeva, S., 2004. Application of the cross wavelet transform and wavelet coherence to geophysical time series. Nonlinear Proc. Geoph. 11, 561–566.
Güssfeldt, P., 1883. Reise in den Andes Chile's und Argentinien's. Verhandlungen der Gesellschaft für Erdkunde zu Berlin, vol. 8, pp. 409–434.
Güssfeldt, P., 1884. Bericht über eine Reise in den centralen chileno-argentinischen Andes. Sitzungsberichte der Kgl. Preuss. Akademie der Wissenschaften zu Berlin XXXIV, pp. 889–929.
Harrison, W., Post, A., 2003. How much do we really know about glacier surging? Ann. Glaciol. 36, 1–6.
Hauthal, R., 1895. Observaciones generales sobre algunos ventisqueros de la Cordillera de los Andes. Rev. Mus. la Plata 6, 109–116.
Holmes, R.L., 1983. Computer-assisted quality control in tree-ring dating and measurement. Tree-Ring Bull. 43, 69–75.
Hurrell, J.W., James, J., Hack, J., Shea, D., Caron, J.M., Rosinski, J., 2008. A new sea surface temperature and sea ice boundary data set for the Community Atmosphere Model. J. Climate. 21, 5145–5153.
IPCC (Intergovernmental Panel on Climate Change), 2001. IPCC Third Assessment Report, Climate Change 2001: The Scientific Basis. Cambridge Univ. Press, Cambridge. 881 pp.
Jones, P.D., Moberg, A., 2003. Hemispheric and large-scale surface air temperature variations: an extensive revision and an update to 2001. J. Climate 16, 206–223.
Juen, I., Georges, C., Kaser, G., 2007. Modelling seasonal runoff variations from glacierized catchment areas in the tropical Cordillera Blanca, Perú. Glob. Planet. Change 58. doi:10.1016/j.gloplacha.2006.11.038.
LaMarche, V.C., Holmes, R.L., Dunwiddie, P.W., Drew, L.G., 1979. Tree-ring Chronologies of the Southern Hemisphere. Chronology Series V., Vol. 2. Laboratory of Tree-Ring Research, University of Arizona, Tucson.
Leiva, J., 1999. Recent fluctuations of the Argentinian glaciers. Glob. Planet. Change 22, 169–177.
Le Quesne, C., Aravena, J.C., Alvarez-García, M.A., Fernández-Prieto, J.A., 2000. Dendrocronología de *Austrocedrus chilensis* en Chile Central. In: Roig, F. (Ed.), Dendrocronología en América Latina. Editorial Nacional de Cuyo, Mendoza, pp. 159–175.
Le Quesne, C., Stahle, D.W., Cleaveland, M.K., Therrell, M.D., Aravena, J.C., Barichivich, J., 2006. Ancient *Austrocedrus* tree-ring chronologies used to reconstruct Central Chile precipitation variability from A.D. 1200 to 2000. J. Climate 19, 5731–5744.
Lliboutry, L., 1956. Nieves y Glaciares de Chile. Fundamentos de Glaciología. Ediciones de la Universidad de Chile, Santiago.
Llorens, R., Leiva, J.C., 1995. Glaciological studies in the high Central Andes using digital processing of satellite images. Mt. Res. Dev. 15 (4), 323–330.
Luckman, B., Villalba, R., 2001. Assessing the synchroneity of glacier fluctuations in the western cordillera of the Americas during the last millennium. In: Markgraf, V. (Ed.), Interhemispheric Climate Linkages. Academic Press, California, pp. 119–140.
Lythe, M., Vaughan, D., the BEDMAP Consortium, 2001. BEDMAP: a new ice thickness and subglacial topographic model of Antarctica. J. Geophys. Res. 106 (B6), 11335–11351.
Mantua, N.J., Hare, S.R., Zhang, Y., Wallace, J.M., Francis, R.C., 1997. A Pacific interdecadal climate oscillation with impacts on salmon production. Bull. Amer. Meteor. Soc. 78, 1069–1079.
Martin, C., 1909. Landeskunde von Chile. L. Friederichsen, Hamburg.
Masiokas, M.H., Villalba, R., Luckman, B.H., Le Quesne, C., Aravena, J.C., 2006. Snowpack variations in the central Andes of Argentina and Chile, 1951–2005: large-scale atmospheric influences and implications for water resources in the region. J. Climate 19, 6334–6352.
Meko, D., Stockton, Ch.W., Boggess, W.R., 1995. The tree-ring record of severe sustained drought. Water Resour. Bull. 31 (5), 789–801.
Montecinos, A., Aceituno, P., 2003. Seasonality of the ENSO-Related rainfall variability in Central Chile and associated circulation anomalies. J. Climate 16, 281–296.
Nogues, A.F., 1894. Note sur un voyaje géologique des thermes de Cauquenes au glacier des ciprés. Actes de la société scientifique du Chili, vol. 3, pp. 148–154.
Norero, A., Bonilla, C., 1999. In: Norero, A., Bonilla, C. (Eds.), Las sequías en Chile, causas consecuencias y mitigación. Pontificia Universidad Católica, Santiago.
Paterson, W., 1994. The Physics of Glaciers. Pergamonn, London.
Peña, H., Nazarala, B., 1987. Snowmelt–runoff simulation model of a central Chile Andean basin with relevant orographic effects. In: Goodison, B.E., Barry, R.G., Dozier, J. (Eds.), Large Scale Effects of Seasonal Snow. IAHS Publication, vol. 166. IAHS Press, pp. 161–172.
Philippi, R.A., 1867. Die Gletscher der Andes. In: Petermann, A. (Ed.), Mittheilungen auf dem Gesammtgebiete der Geographie. Justus Perthes, Gotha, pp. 347–348.
Pissis, J.A., 1860. Descripción topográfica i jeológica de la provincia de Colchagua. Anales de la Universidad de Chile, Tomo XVII, pp. 659–715.
Pissis, J.A., 1875. Atlas de la Geografía Física de la República de Chile. Instituto Geográfico de Paris, Ch. Delagrave, Paris.
Plagemann, A., 1887. Das andine Stromgebiet des Cachapoal. Petermanns Geogr. Mitteillungen. Heft III, Gotha, pp. 65–82.
Quintana, J., 2000. The drought in Chile and la Niña. Drought Network News 12, 3–6.
Quintana, J., 2004. Estudio de los factores que explican la variabilidad de la precipitación en Chile en escalas de tiempo interdecadal. MSc Thesis, Departamento de Geofísica, Universidad de Chile. 88 pp.
Rignot, E., Rivera, A., Casassa, G., 2003. Contribution of the Patagonia icefields of South America to global sea level rise. Science 302, 434–437.
Risopatrón, L., 1924. Diccionario Jeográfico de Chile. Imprenta Universitaria, Santiago.
Rivera, A., Casassa, G., Acuña, C., Lange, H., 2000. Variaciones recientes de glaciares en Chile. Invest. Geogr. 34, 29–60.
Rivera, A., Acuña, C., Casassa, G., Bown, F., 2002. Use of remotely-sensed and field data to estimate the contribution of Chilean glaciers to eustatic sea-level rise. Ann. Glaciol. 34, 367–372.
Rivera, A., Acuña, C., Casassa, G., 2006. Glacier variations in central Chile (32°S–41°S). In: Knight, P.G. (Ed.), Glacier Science and Environmental Change. Blackwell, Oxford, pp. 246–247.
Roig, F.A., 1992. Comparative wood anatomy of Southern South American Cupressaceae. IAWA J. 13, 151–162.
Rosegrant, M., Ringler, C., McKinney, D., Caia, X., Keller, A., Donoso, G., 2000. Integrated economic–hydrologic water modelling at the basin scale: the Maipo river basin. Agr. Econ. 24, 33–46.
Rosenblüth, B., Fuenzalida, H., Aceituno, P., 1997. Recent temperature variations in southern South America. Int. J. Climatol. 17, 67–85.
Röthlisberger, F., 1986. 10000 Jahre Gletschergeshichte der Erde. Verlag Sauerländer, Salzburg.
Schweingruber, F.H., Eckstein, D., Serre-Bachet, F., Bräker, O.U., 1990. Identification, presentation and interpretation of event years and pointer years in dendrochronology. Dendrochronologia 8, 9–38.
Stokes, M.A., Smiley, T.L., 1996. An Introduction to Tree-ring Dating, 2d ed. University of Arizona Press, Tucson.
Torrence, C., Compo, G.P., 1998. A practical guide to wavelet analysis. Bull. Am. Meteor. Soc. 78, 61–79.
Vautard, R., Ghil, M., 1989. Singular spectrum analysis in nonlinear dynamics, with applications to paleoclimatic time series. Physica D 35, 395–424.
Villalba, R., 1994. Climatic fluctuations in mid-latitudes of South America during the last 1000 years: their relationships to the Southern Oscillation (in Spanish). Rev. Chil. Hist. Nat. 67, 453–461.
Villalba, R., Leiva, J.C., Rubulis, S., Suarez, J., Lenzano, L., 1990. Climate, tree-ring and glacial fluctuations in the río Frías Valley, Rio Negro, Argentina. Arct. Alp. Res. 22 (3), 215–232.
Villalba, R., Cook, E.R., D'Arrigo, R.D., Jacoby, G.C., Jones, P.D., Salinger, M.J., Palmer, J., 1997. Sea-level pressure variability around Antarctica since A.D. 1750 inferred from subantarctic tree-ring records. Clim. Dynam. 13, 375–390.
Villalba, R., Cook, E.R., Jacoby, G.C., D' Arrigo, R.D., Veblen, T.T., Jones, P.D., 1998. Tree-ring based reconstructions of northern Patagonia precipitation since AD 1600. Holocene 8, 659–674.